Archives of Civil and Mechanical Engineering (2020) 20:27
https://doi.org/10.1007/s43452-020-00034-0

ORIGINAL ARTICLE

Façade scaffolding behaviour under wind action

Tomasz Lipecki[1] · Paulina Jamińska-Gadomska[1] · Jarosław Bęc[1] · Ewa Błazik-Borowa[1]

Received: 1 October 2019 / Accepted: 29 December 2019 / Published online: 27 February 2020

Abstract
The main objective of the study was to estimate the mean horizontal wind action on a façade scaffolding on the basis of full-scale data. Measurements of climatic parameters were carried out for a number of façade scaffoldings (120 structures) located in Poland over a 30-month period. The measurement points were located on 2–3 deck levels of each structure and at 2–4 points placed in each level. The measurements were carried out 3–4 times during each day for 5 consecutive days. At each point, two components of wind speed were measured: first with the vane probe directed perpendicular to the façade and then parallel to the façade. Each measurement lasted 60 s, and the data were recorded every 1 s. On the basis of wind speeds, a procedure was suggested that enabled estimation of the static wind action on façade scaffoldings. The responses of structures to this action were computed via FEM simulations. The results were compared with those based on the approaches recommended by the wind and scaffolding codes. Initial analyses, illustrated by three scaffoldings without a protective cover, indicated large discrepancies between the approaches and the possibility of wind action, which is not considered in the codes.

Keywords Façade scaffolding · Wind action · In situ measurements · Eurocode · FE analysis

1 Introduction

Scaffoldings are temporary structures mainly erected on construction sites at the walls of new buildings and at the façades of already erected buildings that are under repair, renovation, modernization, etc. Due to their temporary characteristics, scaffoldings are sometimes considered too lightly during design, assembly and exploitation, while any mistake made during any of these stages could cause serious accidents with injuries or even fatalities. A great number of accidents in the construction industry, including fatalities, occur on scaffoldings (mainly falls from a height) and are generated by human or structural mistakes (deficient attachment to the building, defective elements, temporary overloading, deficient bracings) and, to a lesser extent, by wind action. Reports and analyses related to scaffolding failures have been presented for Poland [1], UK [2], USA [3], Hong Kong [4], Scotland [5], the Netherlands [6], and Spain [7]. These works show that all around the world independent of the scaffolding kind or the material used (aluminium, steel, bamboo) there are a large number of serious accidents, including fatalities, associated with scaffoldings. It is impossible to distinguish one decisive reason for failures, but it is clear that wind action is one of the most important factors affecting scaffoldings; wind action could potentially be the primary factor. Therefore, the proper assessment of this load is important during design and exploitation to provide capacity and serviceability limit states.

The design wind action on scaffoldings in Poland (and generally in Europe) is described by two codes, [8, 9], which are supported by the wind code [10]. Wind action should be implemented separately in two different directions: perpendicular to the outer plane of the scaffolding and along the façade of the scaffolding. When the scaffolding is equipped with a protective cover, the characteristics of the wind action are different from those when the scaffolding is not covered. The characteristic value of the resultant wind force, F [kN], is calculated from the following expression:

✉ Tomasz Lipecki
t.lipecki@pollub.pl

Paulina Jamińska-Gadomska
p.jaminska@pollub.pl

Jarosław Bęc
j.bec@pollub.pl

Ewa Błazik-Borowa
e.blazik@pollub.pl

[1] Department of Structural Mechanics, Lublin University of Technology, Lublin, Poland

$$F = c_s \sum_{i=1}^{n} \left(A_i c_{f,i} q_i\right) \quad (1)$$

where A_i is the reference area, c_f is the aerodynamic force coefficient, c_s is the site coefficient, q_i is the characteristic wind velocity pressure, and i is the index of the scaffolding element [8]. The reference area for unclad scaffoldings is the total area of all components projected to the wind in the respective wind direction. The aerodynamic force coefficient takes values with respect to the wind load direction: normal and parallel to the façade. For unclad scaffoldings, there is one value, which is equal to 1.3. More detailed values of c_f for different cross sections of elements are provided by the wind code [10]. The site coefficient describes the position of the scaffolding in relation to the building and should be determined with respect to the wind direction. In the case of unclad scaffoldings, the values are equal to 0.75 (normal) and 1.0 (parallel). Wind action in the direction normal to the unclad scaffolding is defined more precisely in [9]. The code introduces the solidity ratio of the building façade, φ_B, which is the ratio of the façade net area without openings to the total façade area. Taking this into account, the c_s changes linearly from 1.0 for $\varphi_B < 0.1$ to 0.25 for $\varphi_B = 1.0$. Wind velocity pressure depends on the height of the structure above the ground level and changes linearly from 800 Pa for 0 m to 1100 Pa for 24 m. This recommendation [8] should be applied while designing new façade scaffolding systems; otherwise, wind action should be evaluated with [10], according to the mean wind speed vertical profile. The use of the scaffolding codes provides a maximum possible value of pressure without distinction between terrain categories or wind zones. A statistical factor can be considered for the period of working life from the erection to the dismantling of the scaffolding. The factor shall not be less than 0.7 when applied to the wind speed pressure with a 50-year return period [9].

In the literature, there are many papers concerning the mechanical features of entire scaffoldings, single elements or their connections examined in the laboratory or with the use of finite element (FE) analyses (e.g. [11, 12]). The available data about wind action on scaffoldings are very limited and are related mainly to wind tunnel tests of structures with protective covers. A wind tunnel experiment with a scaffolding attached to a medium-height building covered with sheets of 0% porosity was described in [13]. The study focused on buildings with various openings, with different ratios of parts of the façade with openings to the solid façade, and with different arrangements of scaffoldings standing at 1, 2, 3, and 4 walls. The authors measured pressure and then determined the wind force coefficients and stated that these values decreased as the percentage of wall openings increased. The development of the study to the interference effect caused by the neighbouring building, and its influence on the behaviour of scaffoldings placed at 1, 2 or 3 walls was presented in [14]. Irtaza used a wind tunnel experiment and CFD techniques to examine sheet and net clad scaffoldings erected at the full façades of the Silsoe Cube [15]. The authors formulated some recommendations to the code provisions. Wind tunnel tests were performed by Yue et al. [16, 17] on integral-lift scaffoldings used in Asia for high-rise buildings, for which the wind effect can be very significant, especially if the scaffolding is placed over a height of 150 m. Wind pressures on scaffoldings covered with plastic sheets were examined in a wind tunnel by Charuvisit et al. [18]. The scaffolding was placed at one and two walls and partially at two walls. The authors determined the angles of wind attack for which the maximum pressure on scaffolding was obtained. Beale [12] presented an extensive review on the majority of subjects connected with scaffoldings, including wind action on such structures. This review cited many works that were focused on wind action from the conference held by the UK Health and Safety Executive at Bruxton in 1994.

According to the authors' knowledge, there are nearly no data on wind action on scaffolding structures from full-scale experiments in the literature. Tests in wind tunnels focused on scaffoldings covered with protective elements do not fully correspond to the field situation. Protective elements are usually made of light materials that are deformable and susceptible to flutter when exposed to the wind. However, as noted above, rigid panels were used in tunnel tests to model the protective cover. In the case of scaffoldings without a cover, it is very difficult to perform reliable model tests, because the dimensions of the scaffolding and building components differ by several orders of magnitude. After reducing the building-scaffolding system to the size of a model that could be tested in the tunnel, the components have dimensions in millimetres or micrometres. This causes a lack of stability of the scaffolding structure and makes it difficult, or even impossible, to install measurement sensors on the model. Due to such technical difficulties, the only possibility to obtain reasonable results is full-scale research. This study presents such tests on scaffoldings without a protective cover. The extensive measurements of environmental parameters, including wind speed, performed by the authors allow us to expound on the issue of wind loads on temporary beam structures. In the present work, a description of in situ experiments is presented. Then, the proposed estimation of the simplified static wind load is elaborated. The proposal is based on the conversion of wind speed measured on the scaffolding, using data obtained from a nearby meteorological station, to the base wind speed given in the standards. This allowed for comparison of the static response of scaffoldings to wind action determined on the basis of measurements and standards. The application of the procedure is illustrated by

three examples of real scaffolding structures. FE computations are then presented for the responses of these structures to the static wind action based on full-scale data, and based on the scaffolding code and wind code procedures. The issue of the potential wind action not defined by the codes is finally raised.

2 Experiment description

All measurements were performed within the scope of a project focused on the safety of people working on scaffoldings and on the safety of such temporary structures themselves. A total of 120 façade scaffoldings erected all around the territory of Poland were measured with respect to different aspects, including geodesy, instantaneous and permanent loads, and comfort of workers, between April 2016 and November 2018. The results of the measurements of wind speed field with simultaneous measurements of operational load were used to check the ultimate limit state at the maximum load occurring during the week of scaffolding operation and to determine the possibility of structural failure. The measurements were carried out on scaffoldings of various dimensions. The width and height of the objects were in the range of 3.7–75 m and 6–58 m, respectively. The aspect ratio (defined as the height-to-width ratio) was in the range of 0.16–8.65, and the total area of the outer side of the structures was 70.4–1560 m^2.

The important part of the project was microclimate measurements containing wind speed, air pressure, temperature, humidity, insolation and noise. This paper focuses on wind speed measurements performed using the KIMO multifunction instrument AMI 310 and a telescopic vane probe SHT100. The device has a resolution of 0.01 m/s and an accuracy of ± 3% (± 0.1 m/s) for 0.3–3 m/s and ± 1% (± 0.3 m/s) for 3.1–35 m/s. This device could work in a temperature range from − 20 to 80 °C. The main reasons for choosing KIMO devices to measure wind speed were very easy measurements with the possibility of gathering data on a memory card, no need for permanent installation, and the ease of changing the location of measurements. The last point was very important due to a large number of scaffoldings, several locations on every structure, and many repeated measurements. KIMO equipment containing different wind speed devices is commonly used in various in situ experiments, including studies on the environment in commercial airliner cabins [19], the pollution in a residential kitchen [20], the air velocity inside urban vehicular tunnels [21], the air velocity in a ventilated double skin façade [22], and the behaviour of a roof top solar chimney [23].

The climatic measurement points were located on the first, middle, and top deck levels of the scaffolding. In the case of very low structures, the measurement points were on only two levels. The number of locations at each level depended on the size of the scaffolding and varied from 2 to 4. Therefore, the total number of points was between 4 and 12 for each tested structure. The experiment lasted 5 working days at a single scaffolding, and the measurements were repeated 3 or 4 times every day, usually at 8 a.m., 11 a.m., 2 p.m., and sometimes at 5 p.m. During each repetition of measurements and at every point, two components of the horizontal wind speed were recorded. A single measurement lasted 60 s. The data were recorded every 1 s. At a given point, the probe was directed to measure the wind speed acting perpendicularly to the scaffolding (60 s) and then along the façade (60 s), and then the person moved to the next location. An example of the scaffolding with the locations of points and the definition of wind speed axes illustrated by the measurements performed on site are presented in Fig. 1a, b. During the measurements, the influence of the person using a hand-type anemometer was minimized in the construction site environment. Measurements were performed while standing or kneeling motionless with a constant position of the anemometer. Observations during the in situ measurements indicated low sensitivity of results to small changes in the device orientation. Moreover, every person

Fig. 1 Location of measurement points on the scaffolding: **a** diagram of sample locations and directions of wind speed axes, **b** measurements performed on site, and **c** front view of the measurement layout on a single level for a perpendicular component of wind speed (axis 1)

tried to stand at the windward side against the anemometer if the direction of the wind was easy to determine on site. The simplified scheme of the position of the anemometer in the middle of the scaffolding deck is shown in Fig. 1c. The KIMO probe was placed in the middle of the deck span, at a height of 1.4–1.6 m over the deck, and at a distance from the person of approximately 50 cm. The measurements were carried out at a distance from the building wall of approximately 50–80 cm. The majority of scaffolding decks were 70 cm wide, and the anemometer was placed approximately in the middle of the width. The distance from the scaffolding to the building wall varied from 20 to 40 cm. To limit the number of measurements, the vertical component of the wind velocity was not measured. Therefore, the measurements were made at the penultimate or even lower level of decks and always below the level of the building roof. The distance between the device and the roof edge minimized the influence of conical vortices over the roof, which appear mostly for oblique angles. Taking the above assumptions and simplifications into account, the measurements allowed an approximate determination of real wind action on the scaffolding elements based on the data collected within the structure space. For the sake of clarity of the current study, only examples of scaffoldings without a protective cover were chosen. The presence of the cover requires another approach, taking into account its porosity and the additional wind load acting on it.

3 Assessment of the wind load

The proposed procedure of assuming static wind action on façade scaffoldings based on full-scale data consists of the following steps:

1. Data concerning the wind speed collected with KIMO devices were statistically analysed, and 1-min mean values were determined at every measurement point, every hour, and every day of the experiment for two directions: perpendicular and parallel to the façade of the building. The data provided several cases of possible wind action on the structure. The typical 5 days of measurements and 3–4 repeats during a day gave the maximum number of 20 cases. To limit further FE analyses and ensure that the situation was as close to reality as possible, the most unfavourable cases of wind load were chosen taking into account two criteria of choice. The first criterion was the total sum of all magnitudes of the wind speed resultant vectors at a given time of measurement (day and hour). Because a single course of measurements lasted 1 to 1.5 h (4–12 locations on the scaffolding), it was necessary to introduce the assumption that such non-simultaneous measurements could ensure the representative static load of the distribution close to reality. Therefore, the second criterion was based on the analysis of the mean wind speed vectors. These vectors should indicate, taking into account the time shift of the measurements, that they were conducted in more or less constant conditions. This means that the directions of the vectors were similar or that the vectors formed characteristic patterns. According to the authors' opinion, these two criteria allowed minimization of inaccuracies and errors resulting from the non-simultaneous measurements.
2. For the chosen case, the 1-min mean wind speed must be referred to as the 10-min mean wind speed, which is the design value in Eurocodes. The analyses presented by Durst [24] allowed for the conversion of the wind speeds estimated from different averaging times. The gust factor $G_v(T_i/T_{3600})$ defines this conversion, wherein T_{3600} is the 1-hour averaging time and T_i is the other averaging time. Taking T_i as 600 s and 60 s, the gust factor is equal to 1.06 and 1.24, respectively. Thus, $G_v(T_{60}/T_{600})$ can be estimated as 1.17. Other investigations (e.g. [25–29]) and code recommendations [30, 31] gave a recalculated gust factor around this value (approximately 1.12–1.21); so, for further purposes, a value of 1.17 was assumed. This was a rough estimation of the 10-min mean, because the majority of the research mentioned above, especially that presented by Durst [24], was related to open terrain. Scaffoldings usually stand in built-up areas, and the wind flow is changed significantly by the building itself and by neighbouring objects. Exact recalculation between averaging times would require additional measurements on site that were not possible within the scope of the experiment.
3. The wind action on the scaffolding was converted to the design mean wind speed (for example, 22 m/s), taking into account the wind zones in Poland and the ratio of the wind speeds measured on site to those measured at the nearby weather station. It was assumed that the wind speed achieved the design value at the weather station and that it was the reference speed for the scaffolding site. The meteorological station provides values of the wind speed in undisturbed flow, whereas the measurements taken at the construction site describe the flow field, which is the result of this speed and the layout of buildings and other objects between the station and the scaffolding. The available data from meteorological stations in Poland concern the last 10-min mean wind speed from every hour. The value from the weather station corresponding to the hour of chosen measurements was taken as the reference speed.
4. The wind action on the scaffolding according to the measurements was calculated according to the following expression:

$$p_i = qD_i c_{f,i} \tag{2}$$

where $q = 0.5\rho v^2$ is the wind speed pressure based on wind speeds in the chosen case; D_i is the dimension of a particular element, i, when exposed to the wind action; and $c_{f,i}$ are the aerodynamic coefficients of particular elements. The load (in kN/m) was implemented in the FE system, and linear static analysis was performed. The load was applied to the following scaffolding elements subjected to the wind: vertical stands (inner and outer), railings, bracings, and toe-boards (which include thickness of the deck), as shown in Fig. 2. Other elements were omitted due to their low influence on the total load.

Additional cases of load based on code recommendations were also considered. The load was calculated according to Eq. (1). The values of q and c_f were calculated in accordance with the wind code [10], whereas c_s was taken from the scaffolding code, because this is the specific parameter defined only by this code [8, 9]. The reference area was replaced by the diameter (or height for the toe-boards) of the elements to obtain the value in kN/m. When calculating the wind speed pressure, the direction coefficient, c_{dir}, which changes between 0.7 and 1.0, was considered according to National Annex to Eurocode [10]. The load was applied separately in two directions: perpendicular and parallel to the structure according to the scaffolding code rules. All of the above-mentioned elements were loaded in the perpendicular direction, whereas only vertical stands and bracings were loaded in the parallel direction. Additionally, the load defined by Eq. (1) was calculated using the recommendations of scaffolding codes only [8, 9]. It must be emphasized that the use of scaffolding codes is sensible only in the design of new systems of scaffoldings. The value of the wind speed pressure is assumed here at its maximum to cover all possible climate conditions. These values were established as limits for comparisons. In summary, FE linear static analyses were performed for 5 scenarios of the wind load based on case *A*—in situ measurements; case *B*—Eurocode (wind code), perpendicular direction; case *C*—Eurocode (wind code), parallel direction; case *D*—scaffolding code, perpendicular direction; and case *E*—scaffolding code, parallel direction.

To increase the accuracy of the calculations, the values of the measured wind speed were interpolated between measurement levels (Figs. 1a, 4b). For example, if measurements were performed at 3 levels, then 5 levels of different loads were assumed overall. The load based on codes (cases B–E) was determined to be constant at the entire width of scaffolding levels corresponding to levels in case A.

In summary, the wind load determination procedure, based on in situ measurements and on guidelines provided by the wind and scaffolding codes, can be presented in the form of the diagram shown in Fig. 3.

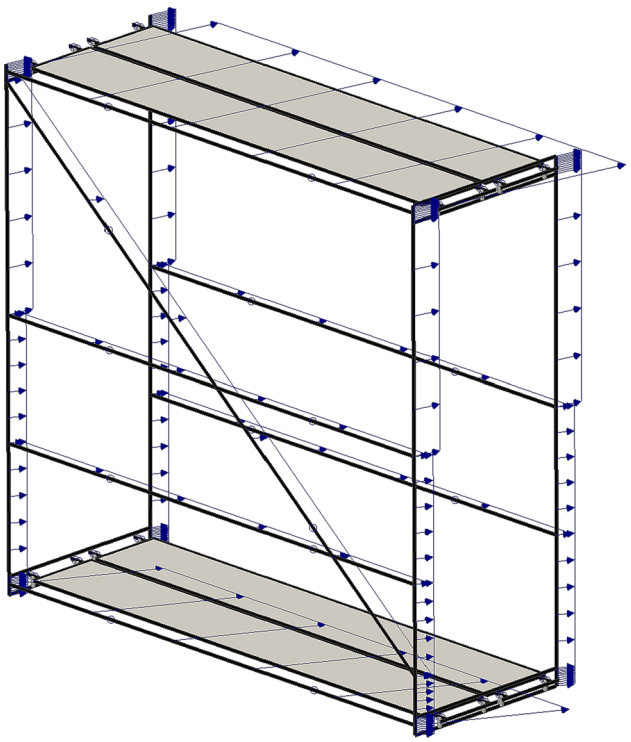

Fig. 2 Continuous load applied to structural elements of the scaffolding in the FE system

4 In situ measurements

Three steel scaffoldings without a protective cover (namely W07, P01, and P10, as shown in Fig. 4) were chosen as examples to illustrate the procedure of estimating the wind load and the static response. The elaborated procedure can be applied to all kinds of scaffoldings without a protective cover. The various heights and widths of the scaffolding do not introduce any changes in the measurement setup and consequently in the calculations. In any case, the load is based on measurements carried out in points defined according to the example in Fig. 1a.

The W07 scaffolding was located in Warsaw in a built-up terrain. This scaffolding had 15 frames and 8 levels of decks. The measured elevation was the southeast one of the large office building. The building was a frame structure with large openings, which resulted in a solidity ratio of 0.3. The climatic measurements were conducted at 12 points over 5 days at 8 a.m., 11 a.m., 3 p.m., and 5 p.m. (with some exceptions due to weather). The most unfavourable case of the wind action, chosen on the basis of the assumptions mentioned in Sect. 3, was on the fifth day, at 11 a.m. The reference 10-min mean wind speed was measured at

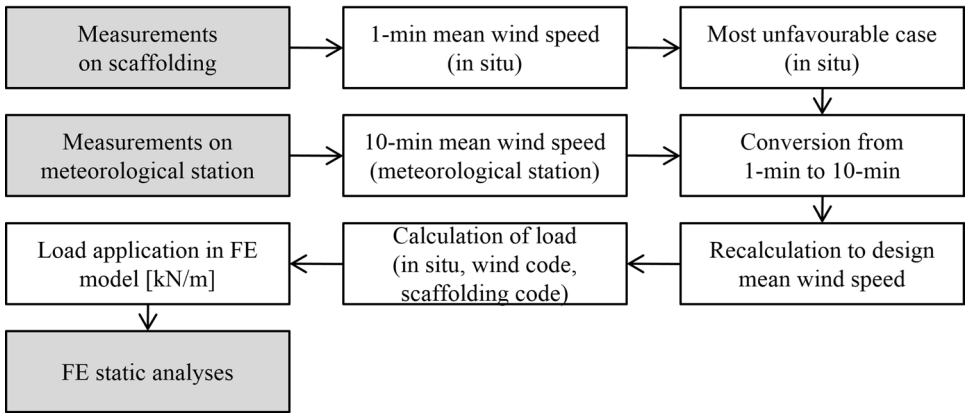

Fig. 3 Scheme of wind load estimation according to the proposed procedure

Fig. 4 Scaffoldings (from left to right) W07, P01, and P10: **a** view and **b** schemes with the location of measurement points

Warsaw–Okęcie Airport weather station, which was approximately 7 km away from the construction site.

The P01 scaffolding was located in Ostrzeszów by the newly constructed residential building standing in the built-up terrain. This scaffolding consisted of 6 frames and 6 levels of wooden decks that were 4.4 cm in thickness. The measured façade was on the north-east side of the solid building. Measurements were carried out in 8 locations over 4 days at 9 a.m., 11 a.m., and 2 p.m. The fifth day was omitted due to weather conditions. For further analyses, the data collected on the second day at 8 a.m. were chosen as the most unfavourable case. Two weather stations, Wieluń-Cewice and Kalisz-Oksywie, were approximately 40 km away from the scaffolding.

The last scaffolding, P10, was located in Krosno in the suburban terrain. This scaffolding had 16 frames and 7 levels of mixed steel, aluminium and wooden decks. The measured elevation was the east-north one of the long office building. The building had a full façade, so the solidity ratio was equal to 1.0. Measurements were carried out in 12 locations over 4 days at 8 a.m., 11 a.m., and 2 p.m. and on one day at 5 p.m. The first day was omitted due to weather conditions. For further analyses, the data collected on the third day at 8 a.m. were chosen. The reference 10-min mean wind speed was measured at the Krosno weather station, which was approximately 3.5 km away from the construction site.

The ranges of the wind velocity characteristics in the chosen time are collected in Table 1. These ranges are based on

Table 1 Ranges of wind speed characteristics in the chosen time of the measurements (m/s)

	$v_{1,m}$	$v_{2,m}$	σ_1	σ_2	v_1	v_2
W07	0.57–3.39	−1.11–2.22	0.22–0.88	0.23–1.47	−0.62–5.48	−2.01–4.90
P01	−0.44–1.22	0.84–3.06	0.19–0.42	0.52–1.31	−1.08–2.42	−1.06–4.95
P10	−0.09–2.17	−2.46–0.42	0.09–0.70	0.23–2.31	−1.31–3.69	−5.00–2.94

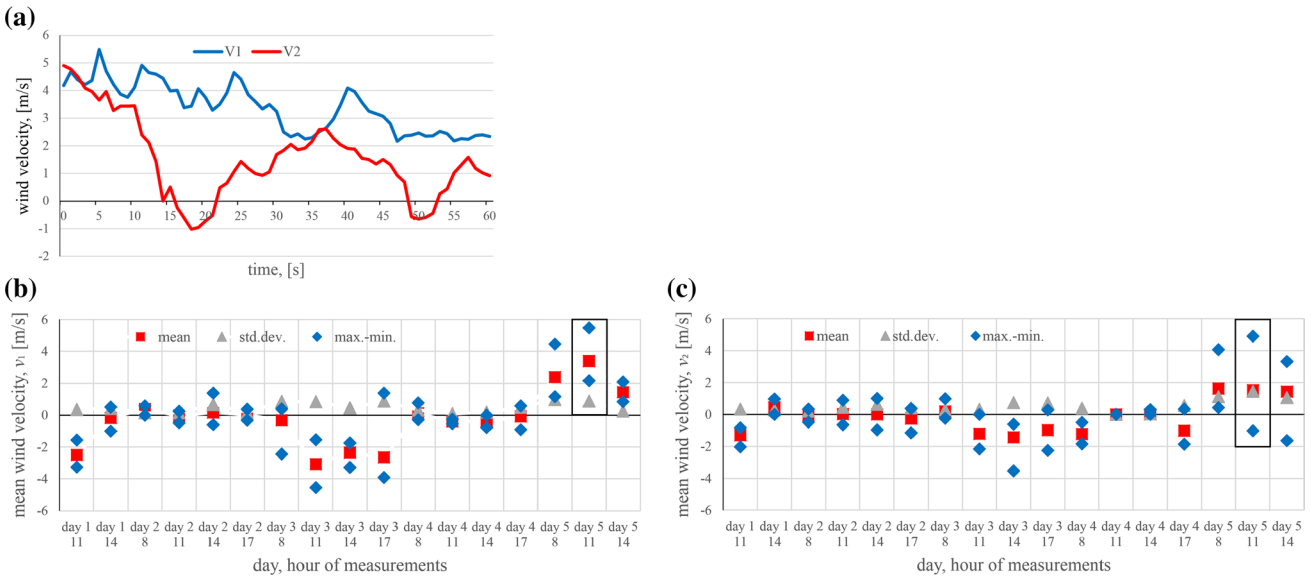

Fig. 5 Wind speeds v_1 and v_2: **a** over 1 min with 1 s of sampling, and **b**, **c** 1-min mean, standard deviation, range of maximum and minimum 1-s values. Data from the top, right measurement point of structure W07

data from all measurement points and are related to 1-min mean $v_{1,m}$ and $v_{2,m}$, 1-s instantaneous v_1 and v_2, and standard deviations σ_1 and σ_2 for the perpendicular (1) and parallel (2) directions of wind velocity, respectively. An example of a 1-min record with 1 s of sampling, registered at the top right point of scaffolding W07, is shown in Fig. 5a. The mean wind speed, its standard deviation, and the range of instantaneous speeds (max–min) for this point are presented in Fig. 5b for every hour and day of measurements. More detailed information about this case study can be found in [32].

Additional assumptions based on in situ observations and code provisions are listed in Table 2. The design values of wind speed were 22 m/s, and the results from the scaffoldings were recalculated to this value. The directional coefficient c_{dir} was estimated from the National Annex to Eurocode on the basis of the mean wind speed direction measured at the nearby weather station at the time of the measurements. The patterns of resultant wind speed vectors in the chosen cases acting on the measurement points are presented in Fig. 6. The values of speeds were recalculated to the design ones, and then the wind load per unit length acting on the scaffolding elements was estimated according to the procedure described in Sect. 3.

Table 2 Wind action assumptions

	W07	P01	P_10
Mean wind speed at the weather station	4 m/s	5 m/s	4 m/s
Wind load zone	1	1	3
Terrain category	4	4	2
Solidity ratio, φ_{B}	0.3	1	1
Site coefficient, c_{s}	0.833	0.25	0.25
Directional coefficient, c_{dir}	SE: 0.7	ESE: 0.7	S: 1.0

5 FE modelling

The results of the in situ measurements were wind speeds and directions in several locations. The actual full-scale wind action did not coincide with the directions recommended by the standards, so it was difficult to compare the determined loads directly with each other. Therefore, the responses of each structure to the static wind action based on various approaches were compared. For this purpose, FE models of the structures were created. An example of

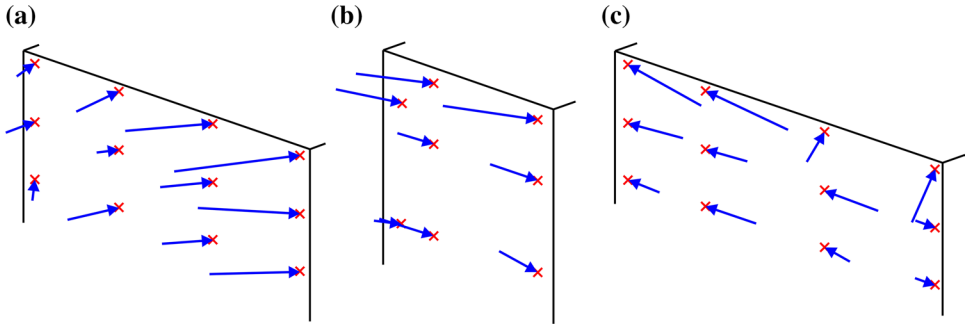

Fig. 6 Resultant directions of 1-min wind speed vectors for chosen cases of wind load: **a** W07, **b** P01, and **c** P10

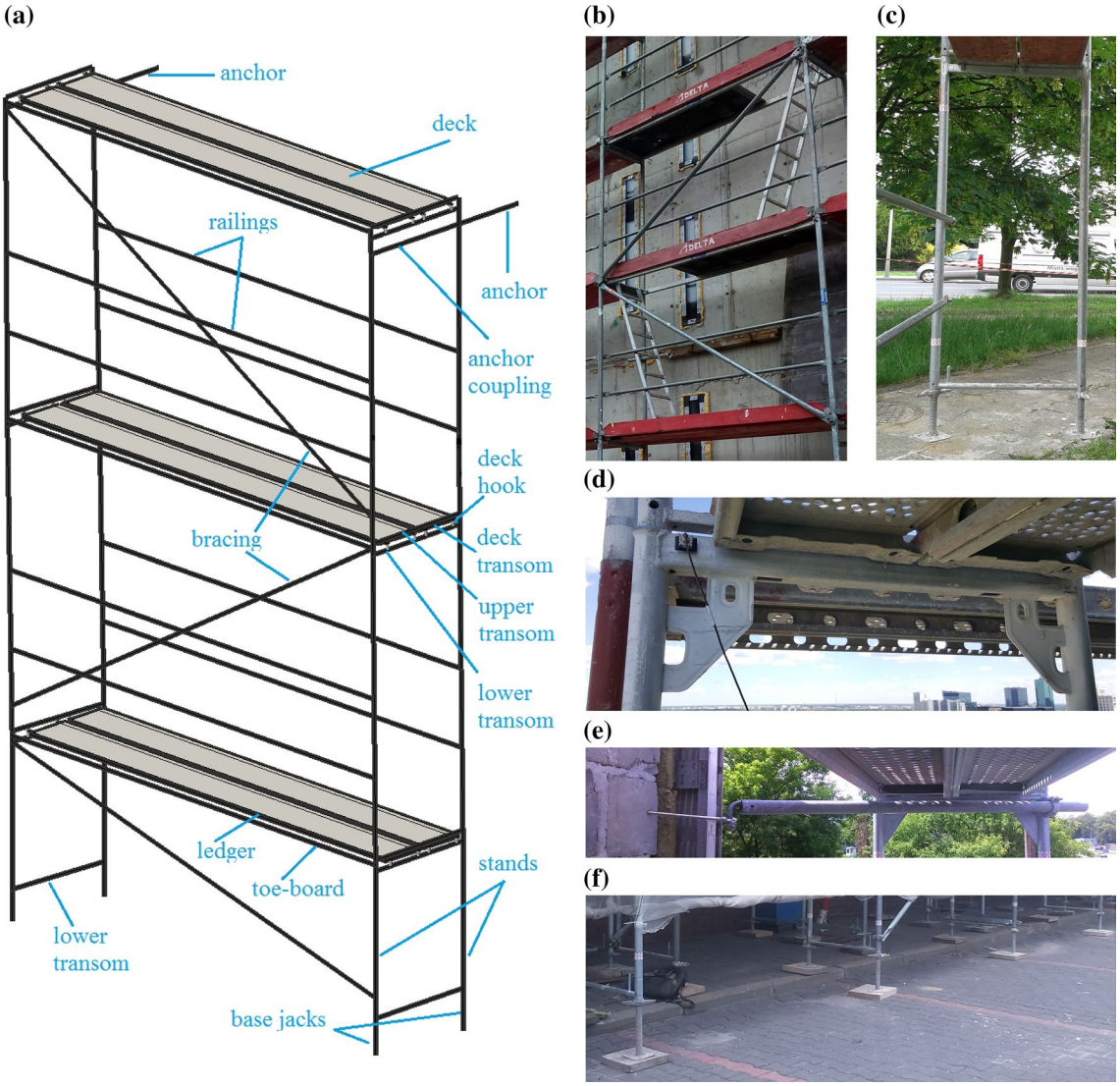

Fig. 7 Elements used in scaffolding systems: **a** description, **b** main elements, **c** single frame with lower and upper transoms, **d** upper transom and its connection with steel decks and gusset plates, **e** anchors and anchor couplings, and **f** base jacks

scaffolding composed of typical elements commonly used in Europe is presented in Fig. 7.

Cross sections of the scaffolding elements were based on the in situ observations and the producer's catalogues. Geodesic measurements were carried out for all structures, and the real locations of their nodes (connections between frames and decks) in space were established. The correct position of the connections between the upper u-sections and the lower transoms, as well as the bracings and railings, were modelled on the basis of the in situ inventory control. The created FE models represented "real" scaffoldings during their work on the construction site. Not all elements were modelled directly. The mass density of the frame was increased by additional weights of gusset plates, railing edges, and welded studs (elements in Fig. 7d), for which the characteristics were taken from the in situ observations and producer's catalogues. A simplified structure of the decks was used, which consisted of plate elements with transoms and ledgers and mounting hooks. The weight and stiffness of these simplified elements were previously analysed in detail to reflect the behaviour of real decks [33]. In the case of P01, the decks were made of wood and were not simplified but modelled directly as plate elements with anisotropic features. All the elements other than the decks were modelled as beams. The basic elements of all scaffoldings had the following shapes and dimensions: stands—pipes, $D = 48.3$ mm; railings—pipes, $D = 38$ mm; bracings—pipes, $D = 42$ mm; and wooden toe-boards—rectangular cross section of 15 cm × 3 cm. The anchorage system and boundary conditions in the supports and connections between particular elements were set according to in situ observations. Rigid and hinge connections were applied in the models. All models were validated by in situ measurements. Free vibrations tests were performed on all scaffoldings with excited forces applied at different points and directions. Accelerations of vibrations were measured in several locations. Spectral analysis was performed on the acceleration time histories, which provided the dynamic characteristics of the structure. A comparison of the results from the FE modal analysis and full-scale measurements indicated that some models had to be slightly improved. In practice, this meant that some DOFs in particular supports were released or masses in specified locations were added in the FE models. Additional validation of the models was based on the full-scale measurement of axial forces in the chosen stands. The characteristics of changes introduced to the model were different in particular cases, but finally, the frequencies and mode shapes obtained in the FE computations were close to those from the full-scale. More details of FE modelling of scaffoldings can be found in [34]. Clearances in the connections between elements were not modelled. Scaffoldings as temporary structures are used several times, so the clearances between the elements and the inaccuracies arising in each subsequent assembly are unavoidable. The clearances mainly influenced the damping of the structure, which was also observed during the in situ dynamic tests of the excited vibrations. Full-scale observations of the behaviour of scaffoldings allowed us to conclude that the connections, in static load conditions, basically blocked the possibility of movement, and the use of the hinge connection was justified. This was mainly related to the connections between the anchor coupling with the hook and the anchor eye bolt. An additional reason why the clearances were not modelled in the whole structure was the excessive computing power necessary to carry out the correct calculations with such boundary conditions. The authors assumed that this was unnecessary for the main purpose of the study. The FE models of the three structures are presented in Fig. 8.

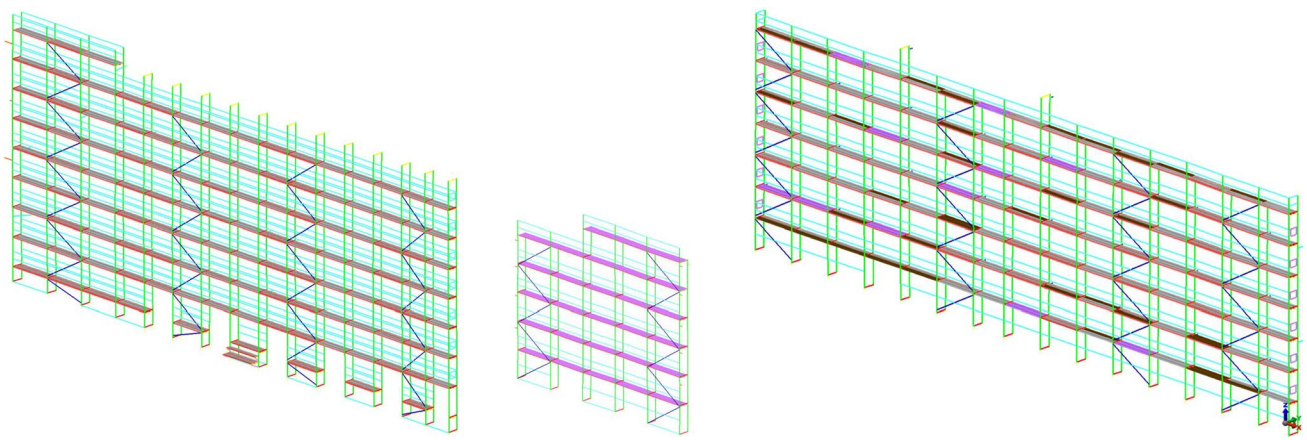

Fig. 8 FE models of W07 (left), P01 (middle), and P10 (right)

Table 3 Magnitude of maximum displacements for load cases *A*–*E*

	Magnitude of maximum displacements (cm)				
	Case *A*	Case *B*	Case *C*	Case *D*	Case *E*
W07	0.88	2.00	0.38	5.01	1.23
P01	0.29	0.17	0.42	0.35	1.34
P10	0.62	0.89	2.37	0.97	3.80

6 Discussion of the results

All FE static analyses were carried out to check the influence of wind loads only, so the other influences, including deadweight, were not considered. The chosen load systems (comp. Fig. 6) were implemented in the models. The magnitudes of the maximum displacement are collected in Table 3, and the example deformation forms of the W07 scaffolding are presented in Fig. 9. The scale due to the legibility is not maintained between figures, and the deformations are largely scaled-up. The forms of deformation were the same for wind and scaffolding code approaches (cases *B* and *D* and cases *C* and *E*, respectively). Larger values of displacements were obtained in cases *C* and *E* due to higher multipliers of load derived on the basis of the scaffolding code. When considering W07, the form of deformation in case *A* was roughly similar to that in cases *B* and *D*, because the directions of forces were close to perpendicular to the façade (Fig. 6a). The displacements obtained for perpendicular loads were higher than those for parallel loads, which was different for scaffoldings P01 and P10. In general, the wind action induced small displacements of structure P01, which suggested high stiffness of the entire structure. Slightly higher displacements were obtained for parallel loads (cases *C* and *E*) in P01, and significantly higher in P10. The components of the displacement vector were the largest along axes 1 or 2 in accordance with the load direction for all structures.

There were different locations of maximum displacements between the cases of loads. For W07, the maximum displacements occurred in the first from the right outer top stand (case *A*), in the sixth from the right outer top stand (cases *B* and *D*), and in the first from the left outer top stand (cases *C* and *E*). Considering P01, the maximum displacements were observed in the top right outer stand (case *A*), in the third from the left outer stand at the third level of decks (cases *B* and *D*), and in the fourth from the left inner lower stand, which was due to released DOF along the façade (cases *C* and *E*). The same behaviour was observed for P10, in which the locations were in the fifth from the left outer top stand (case *A*), in the fourth from the right outer top stand (cases *B* and *D*) and in the eighth from the right inner top stand (cases *C* and *E*).

The axial force, torque, bending moments, and normal stresses in the beam elements were compared between the cases of loads. The worst normal stresses were calculated according to the formula:

$$\sigma = \frac{|N|}{A_c} + \frac{|M_2|}{W_2} + \frac{|M_3|}{W_3} \tag{3}$$

where A_c is the cross sectional area, W_2 and W_3 are the sectional moduli, N is the axial force, and M_2 and M_3 are the bending moments against two axes of the cross section.

The extreme values of σ in the main elements are shown in Fig. 10. Low values of stress were found in the railings, bracings, and toe-boards, as could be expected, because these are not structural elements. In the case of bracings, the values of normal forces are important. If there is a high axial force in a bracing, then there is a possibility that the bracing will fall out of the connection or cut the mandrel depending on the scaffolding system used. Low stresses were also found in the ledgers under the deck, which are structural elements but are rigidly connected to the steel decks. The anchors also had relatively low stresses, but for

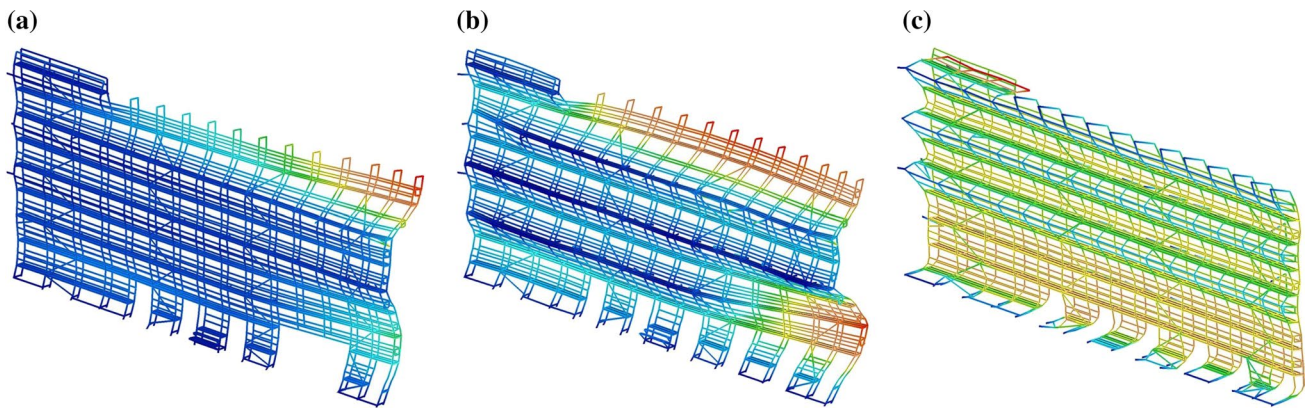

Fig. 9 Forms of deformation in W07 obtained in static analysis under wind action in cases **a** A, **b** B, and **c** C

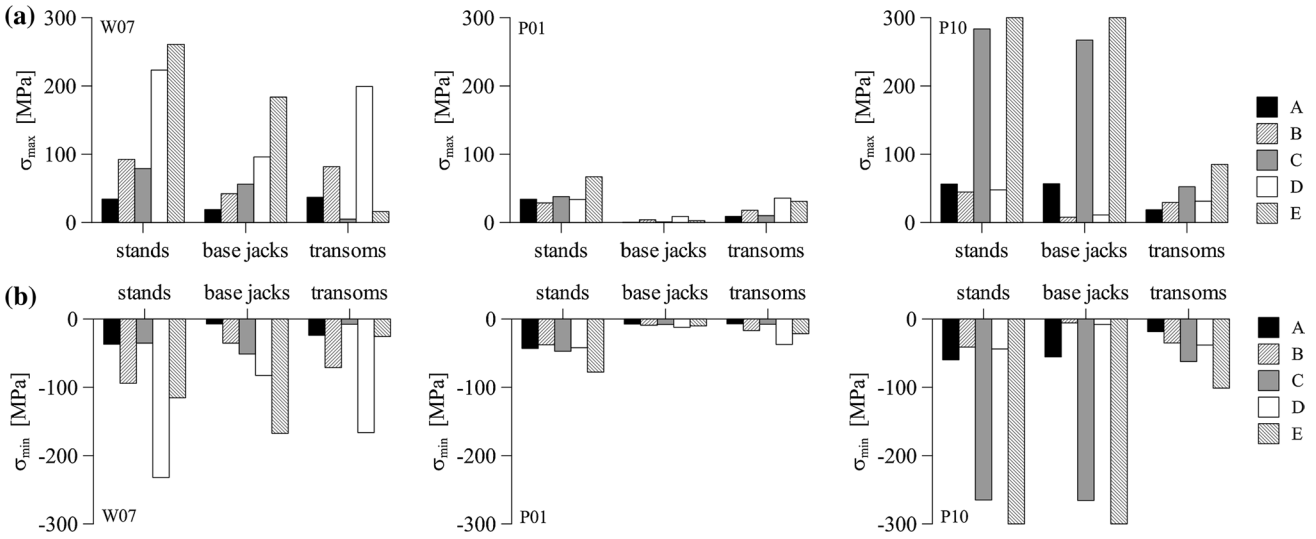

Fig. 10 Normal stresses in scaffolding elements, cases *A*–*E*: **a** maximum values and **b** minimum values

these elements, normal forces are also important. These normal forces are equal to the forces pulling the anchor out of the façade. The maximum axial force in a standard anchor, permitted by Polish regulations, is 2.5 kN. It is possible to increase this value by using glued anchors. Then, the load capacity of the coupling between the anchor and the stand is a limit for its use. In most systems, the maximum force is defined as 9 kN. Standard anchors were used in all constructs described in this paper. Locally, in stands and base jacks, the stresses were close to limit values or even exceeded them in the case of the load calculated on the basis of the scaffolding code (Fig. 10, P10). This code assigned to the newly designed scaffolding systems does not consider terrain, wind zone and temporary or seasonal factors, which results in higher loads. The limited stresses that can be accepted for steel scaffolding elements are usually in the range of 260–320 MPa; as shown in Fig. 10, an average of 300 MPa is used as the upper limit. Extreme values of normal stresses are additionally collected in Table 4. Accepting the lowest value of 260 MPa as the limit, the exceeding values are designated with italic values in the table, and the values close to this limit, i.e. 80–100% of this limit, are designated with bold fonts. The bearing capacity is exceeded only in the case of the wind load directed parallel to the façade (P10, cases *C* and *E*).

Detailed comparisons of the internal forces N, M_2, and M_3 for the chosen elements with the largest effort and the axial forces N in the bracings and anchors are presented in Table 5. Tensile and compressive axial forces had very similar values, and only extreme forces are shown. Only absolute extreme values of bending moments without distinction of their direction are noted. The moments M_2 and M_3 were relatively low. However, considering the values of the sectional moduli for the thin pipe elements, these moments could produce larger stresses than the axial forces. In the case of axial forces in the anchors, values exceeding 2.5 kN and close to the limit were found (italic values and bold font, respectively).

Analysing the distribution of the extreme worst normal stresses with respect to the forces and moments in W07, it was noticed that their locations were different from case to case. Extreme values of σ were in the elements at the right side of the structure and roughly in accordance with the deformation shape (cases *A*, *B*, and *D*). For example, extreme values of σ were located in the second stand from

Table 4 Extreme normal stresses in scaffolding elements [MPa]

	Stands			Base jacks			Upper/lower transoms		
	W07	P01	P10	W07	P01	P10	W07	P01	P10
A	−36.93	−43.03	−59.66	19.06	−7.32	56.77	36.98	8.96	18.61
B	−94.10	−37.67	44.57	42.10	−9.05	7.71	81.74	17.89	−35.00
C	78.90	−47.18	*283.49*	56.18	−8.02	*267.10*	−7.69	10.05	−62.23
D	**−232.06**	−42.07	47.77	96.02	−12.11	11.06	199.24	−37.17	−38.01
E	**260.76**	−77.67	*472.20*	183.62	−10.09	*444.00*	−25.54	30.93	−101.13

Table 5 Extreme internal axial forces and bending moments in scaffolding elements

	Stands			Base jacks			Upper/lower transoms			Anchors			Bracings		
	W07	P01	P10	W07	P01	P10	W07	P01	P10	W07	P01	P10	W07	P01	P10
N [kN]															
A	1.21	−2.50	2.53	1.22	−2.28	2.53	0.96	0.19	−0.25	−1.05	0.23	−0.28	0.44	0.64	−1.17
B	2.57	−2.18	−0.90	2.57	−1.99	−0.90	3.34	−0.45	−1.92	*−3.28*	−0.57	**−2.11**	−0.35	0.55	−0.05
C	−1.33	−2.47	−9.30	−1.33	−2.44	−9.30	0.12	0.26	−0.24	−0.11	0.31	0.18	1.47	−0.91	5.69
D	6.33	−2.14	−0.95	6.33	−1.82	−0.95	7.83	−0.95	−2.01	*−7.89*	−1.22	**−2.22**	−0.86	0.66	−0.06
E	−4.40	−3.10	−17.90	−4.42	−3.10	−14.90	−0.41	0.78	−0.39	−0.36	0.95	0.29	4.82	−1.85	2.71
M_2 [kN m]															
A	0.09	0.15	0.22	0.03	0.00	0.11	0.12	0.03	0.11	–	–	–	–	–	–
B	0.12	0.12	0.06	0.01	0.00	0.00	0.38	0.04	0.23	–	–	–	–	–	–
C	0.31	0.17	1.08	0.12	0.00	0.53	0.06	0.03	0.49	–	–	–	–	–	–
D	0.27	0.12	0.06	0.02	0.00	0.00	0.88	0.08	0.24	–	–	–	–	–	–
E	1.03	0.30	1.81	0.40	0.00	0.88	0.18	0.06	0.80	–	–	–	–	–	–
M_3 [kN m]															
A	0.13	0.03	0.05	0.01	0.00	0.00	0.14	0.03	0.07	–	–	–	–	–	–
B	0.37	0.06	0.18	0.08	0.01	0.01	0.40	0.05	0.20	–	–	–	–	–	–
C	0.01	0.04	0.03	0.00	0.00	0.01	0.01	0.04	0.05	–	–	–	–	–	–
D	0.88	0.14	0.19	0.18	0.02	0.02	0.94	0.11	0.22	–	–	–	–	–	–
E	0.04	0.11	0.05	0.01	0.01	0.01	0.05	0.13	0.09	–	–	–	–	–	–

the right at the seventh level of decks (min.) and in the upper transom under this deck (max.) in case *A*. The location of extreme internal forces N, M_2, and M_3 and particular components of normal stresses (Eq. 3) were in different elements of the structure. Similar observations were also applied to the results of computations based on codes—cases *B* and *D* and cases *C* and *E*. In general, it was very difficult to predict the most stressed elements, the locations of the worst stresses, and the corresponding internal forces in the entire structure. Considering stands in case *A* under wind loading, the extreme worst normal stresses in these elements were equal to 34.20 MPa (max.) and − 36.93 MPa (min.). The stress components produced by the axial force N and the bending moments M_2 and M_3 (Eq. 3) in the location of extreme stresses were equal to 1.26 MPa, 3.90 MPa, 29.03 MPa (max.) and − 1.35 MPa, − 3.70 MPa, − 31.88 MPa (min.), respectively. Thus, the influence of bending moments was the largest for these elements. When considering internal forces N, M_2, and M_3 in these locations, they were equal to 0.489 kN, 1.629×10^{-2} kN m, and 0.121 kN m (max.) and − 0.520 kN, -1.545×10^{-2} kN m, − 0.133 kN m (min.).

For comparison, a static analysis with the deadweight only was performed, and it gave the maximum displacement equal to 0.32 cm in the dominant vertical direction and the worst normal stress equal to − 21.38 MPa.

The load capacity was not exceeded in any element of scaffolding P01. The extreme worst stresses were at a reasonable level, with the largest values in the stands. The distribution of extreme values in the stands was different for particular load cases. However, the stresses in the stands produced by axial forces were always several times smaller than those produced by bending moments acting in the direction parallel to the façade. The stresses caused by bending moments acting to or from the façade were also significantly smaller. Cases *B* and *D* were the exceptions in which the axial stresses were also small, but the bending stresses in the two directions were comparable. In general, the response of P01 was the largest for case *E*, but when comparing case *A* (measurements) with cases *B*, *C*, and *D*, the discrepancies were small. The stresses were higher in case *A* than in case *B* and comparable with cases *C* and *D* in some elements. Such results indicate that the approach to the design of the scaffoldings in the codes could not cover situations that are potentially dangerous to the structure.

The values of displacements and stresses caused by the wind action were slightly higher when compared to the values obtained in the analysis with deadweight only. The maximum displacement under deadweight was 0.3 cm in the vertical direction, and the minimum worst normal stress in the stands was − 39.0 MPa.

In elements of structure P10, the load capacity was exceeded at a parallel wind load based on the scaffolding code (case *E*). Excessively high stresses appeared in the stands and base jacks. The results in case *C* also gave stresses at their limit level. Stresses were significantly lower when considering perpendicular load (cases *B* and *D*) or load based on measurements (case *A*), which was nearly parallel to the façade with some disturbances

close to the edge (Fig. 6c). In the stands, the stresses were approximately at 20% of the load capacity, which was equal to 260 MPa. Calculations based on measurements gave a higher response when compared to calculations assuming perpendicular loads, especially in base jacks. Extreme normal stresses in the stands in case *A* were located in the fifth and the eleventh from the right bottom outer elements and were equal to 56.3 MPa and − 59.66 MPa, respectively. Particular components of Eq. (3) in these locations were equal to 6.33 MPa, 49.89 MPa, and 0.08 MPa (max.) and − 6.48 MPa, − 53.14 MPa, and − 0.32 MPa (min.), whereas internal forces and moments N, M_2, and M_3, which produced these stresses, took the following values: 2.447 kN, 0.208 kN m, and 3.482×10^{-4} kN m (max.) and − 2.58 kN, − 0.222 kN m, and 1.297×10^{-4} kN m (min.), respectively.

The total maximum displacement under deadweight was nearly negligible at 0.05 cm, and the minimum worst normal stress in the stands was − 17.49 MPa.

Different locations of extreme normal stresses in the stands and the most stressed anchors are presented in Fig. 11 for all three structures and load cases *A*–*E*.

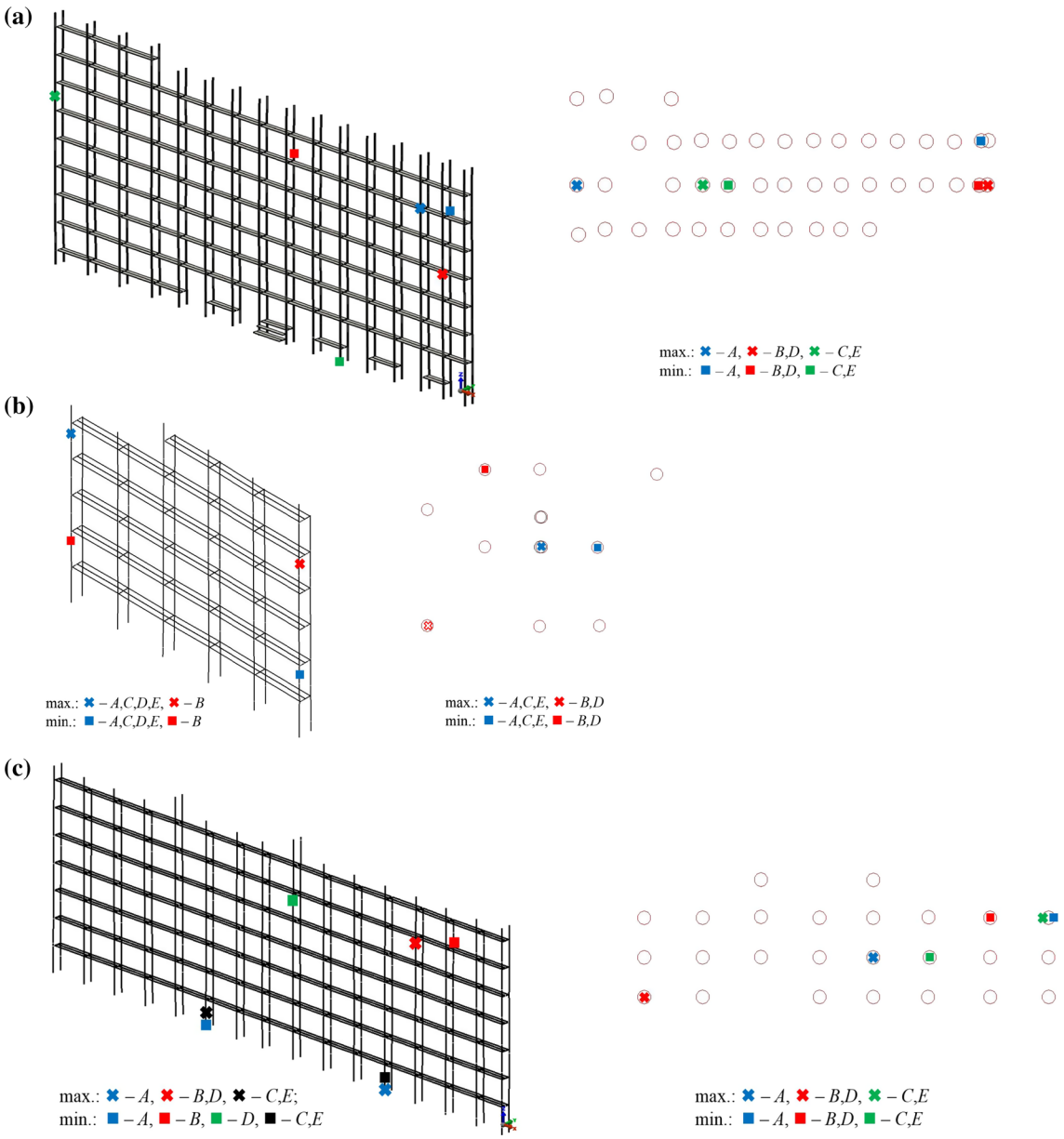

Fig. 11 Locations of extreme normal stresses in the stands (left) and anchors in front view of the scaffoldings (right): **a** W07, **b** P01, and **c** P10

7 Conclusions

In this paper, a procedure was presented for estimating the wind load acting on façade scaffolding structures without a protective cover based on in situ measurements. Additionally, scaffolding and wind code approaches were discussed. The results of FE static analyses of three examples of façade scaffoldings illustrated the problem. The first of them (W07) was erected at a building with large openings, whereas the other two (P01 and P10) stood at solid buildings. In the majority of cases, the code recommendations remained conservative—like for W07, where the results based on in situ measurements were much lower than the other ones. In contrast, the response of P01 was comparable with those obtained in accordance with the Eurocode or as in the case of P10 exceeded it. Basically, the scaffolding code gave the highest stress values in all cases, but it was intended for the design of new scaffolding systems and not for the particular scaffolding setting at the construction site. In summary, the displacements, stresses, and internal forces in all three scaffoldings were rather low for wind loads based on measurements (case *A*) and were comparable, or in a few cases exceeding, the ones obtained for loads based on Eurocode (cases *B* and *C*). Taking into account deadweight or additional operational loads, the stresses can increase significantly. However, in general, the wind mainly affects the anchors, so these loads cause the greatest effort in the stands located in the bottom frames and in the base jacks. The detailed analyses of the location of extreme stresses in the entire structure caused by the wind load indicated their different distributions when compared to the codes approaches of normal and parallel loads. This could induce larger effort of other elements than those identified with code approaches.

In the authors' opinion, the presented procedure of load assessment based on in situ experiments can approximate the real load. Two components of the horizontal wind speed were measured inside the scaffolding structure: in the middle of the deck and in the middle of the level height. Thus, the forces applied to the particular elements of the FE model roughly represented real wind forces. The influence of the location of the scaffolding against the building itself and against the whole system of neighbouring buildings is included in this procedure. On the other hand, the procedure is burdened with some uncertainty due to the reasons described in Sect. 3 and is also affected by a number of factors, the most important of which is the lack of precision of full-scale measurements performed with the used devices.

Acknowledgements The paper was prepared as a part of the project supported by the National Centre for Research and Development within an Applied Research Programme (Agreement No. PBS3/A2/19/2015 "Modelling of Risk Assessment of Construction Disasters, Accidents and Dangerous Incidents at Workplaces Using Scaffoldings").

Funding None.

Compliance with ethical standards

Conflict of interest The authors declared that they have no conflicts of interest.

Ethical approval Authors state that the research was conducted according to ethical standards.

References

1. Błazik-Borowa E, Szer J. The analysis of the stages of scaffolding "life" with regard to the decrease in the hazard at building works. Arch Civ Mech Eng. 2015;15:516–24. https://doi.org/10.1016/j.acme.2014.09.009.
2. Whitaker SM, Graves RJ, James M, McCann P. Safety with access scaffolds: development of a prototype decision aid based on accident analysis. J Saf Res. 2003;34:249–61. https://doi.org/10.1016/S0022-4375(03)00025-2.
3. Halperin KM, McCann M. An evaluation of scaffold safety at construction sites. J Saf Res. 2004;35:141–50. https://doi.org/10.1016/j.jsr.2003.11.004.
4. Fang D, Shen Q, Wu S, Liu G. A comprehensive framework for assessing and selecting appropriate scaffolding based on analytic hierarchy process. J Saf Res. 2003;34:589–96. https://doi.org/10.1016/j.jsr.2003.05.008.
5. Cameron I, Hare B, Davies R. Fatal and major construction accidents: a comparison between Scotland and the rest of Great Britain. Saf Sci. 2008;46:692–708. https://doi.org/10.1016/j.ssci.2007.06.007.
6. Bellamy LJ. Exploring the relationship between major hazard, fatal and non-fatal accidents through outcomes and causes. Saf Sci. 2015;71:93–103. https://doi.org/10.1016/j.ssci.2014.02.009.
7. Rubio-Romero JC, Gámez MCR, Carrillo-Castrillo JA. Analysis of the safety conditions of scaffolding on construction sites. Saf Sci. 2013;55:160–4. https://doi.org/10.1016/j.ssci.2013.01.006.
8. EN12810-1. Façade scaffolds made of prefabricated components—Part 1: Product specifications, European Committee for Standardization, Brussels, Belgium, 2002.
9. EN12811-1. Temporary works equipment—Part 1: Scaffolds—Performance requirements and general design, European Committee for Standardization, Brussels, Belgium, 2003.

10. EN1991-1-4. Eurocode 1: Actions on structures—Part 1–4: General actions—Wind actions, European Committee for Standardization, Brussels, Belgium, 2008.
11. Pieńko M, Błazik-Borowa E. Numerical analysis of load-bearing capacity of modular scaffolding nodes. Eng Struct. 2013;48:1–9. https://doi.org/10.1016/j.engstruct.2012.08.028.
12. Beale RG. Scaffold research—a review. J Constr Steel Res. 2014;98:188–200. https://doi.org/10.1016/j.jcsr.2014.01.016.
13. Wang F, Tamura Y, Yoshida A. Wind loads on clad scaffolding with different geometries and building opening ratios. J Wind Eng Ind Aerodyn. 2013;120:37–50. https://doi.org/10.1016/j.jweia.2013.06.015.
14. Wang F, Tamura Y, Yoshida A. Interference effects of a neighboring building on wind loads on scaffolding. J Wind Eng Ind Aerodyn. 2014;125:1–12. https://doi.org/10.1016/j.jweia.2013.11.009.
15. Irtaza H, Beale RG, Godley MHR. A wind-tunnel investigation into the pressure distribution around sheet-clad scaffolds. J Wind Eng Ind Aerodyn. 2012;103:86–95. https://doi.org/10.1016/j.jweia.2012.03.004.
16. Yue F, Yuan Y, Li G, Ye K, Chen Z, Wang Z. Wind load on integral-lift scaffolds for tall building construction. J Struct Eng. 2005;131:816–24. https://doi.org/10.1061/(ASCE)0733-9445(2005)131:5(816).
17. Yue F, Li GQ, Yuan Y. Design methods of integral-lift tubular steel scaffolds for high-rise building construction. Struct Des Tall Spec Build. 2012;21:46–56. https://doi.org/10.1002/tal.635.
18. Charuvisit S, Hino Y, Ohdo K, Maruta E, Kanda M. Wind tunnel experiment on wind pressures acting on the scaffolds in strong winds. J Wind Eng JAWE. 2007;32:1–10. https://doi.org/10.5359/jwe.32.1.
19. Lei L, Wang S, Zhang TT. Inverse design of underfloor heating power rates and air-supply temperature for an aircraft cabin. Appl Therm Eng. 2016;95:70–8. https://doi.org/10.1016/j.applthermaleng.2015.11.049.
20. Zhou B, Chen F, Dong Z, Nielsen PV. Study on pollution control in residential kitchen based on the push-pull ventilation system. Build Environ. 2016;107:99–112. https://doi.org/10.1016/j.buildenv.2016.07.022.
21. Tong Y, Wang X, Zhai J, Niu X, Liu LL. Theoretical predictions and field measurements for potential natural ventilation in urban vehicular tunnels with roof openings. Build Environ. 2014;82:450–8. https://doi.org/10.1016/j.buildenv.2014.09.003.
22. de Gracia A, Navarro L, Castell A, Ruiz-Pardo Á, Alvárez S, Cabeza LF. Experimental study of a ventilated facade with PCM during winter period. Energy Build. 2013;58:324–32. https://doi.org/10.1016/j.enbuild.2012.10.026.
23. Al-Kayiem HH, Sreejaya KV, Gilani SIU-H. Mathematical analysis of the influence of the chimney height and collector area on the performance of a roof top solar chimney. Energy Build. 2014;68:305–11. https://doi.org/10.1016/j.enbuild.2013.09.021.
24. Durst CS. Wind speeds over short periods of time. Meteorol Mag. 1960;89:181–6.
25. Ashcroft J. The relationship between the gust ratio, terrain roughness, gust duration and the hourly mean wind speed. J Wind Eng Ind Aerodyn. 1994;53:331–55.
26. Ishizaki H. Wind profiles, turbulence intensities and gust factors for design in typhoon-prone regions. J Wind Eng Ind Aerodyn. 1983;13:55–66.
27. Krayer WR, Marshall RD. Gust factors applied to hurricane winds. Bull Am Meteorol Soc. 1992;73:613–7.
28. Mitsuta Y, Tsukamoto O. Studies on spatial structure of wind gust. J Appl Meteorol. 1989;28:1155–61.
29. Harper BA, Kepert JD, Ginger JD. Guidelines for converting between various wind averaging periods in tropical cyclone conditions. Geneva, Switzerland: World Meteorological Organization, 2010.
30. ISO 4354:2012. Wind actions on structures, ISO, Geneva, Switzerland, 2009.
31. ESDU83045. Strong winds in the atmospheric boundary layer. II: Discrete gust speeds, Engineering Science Data Unit, London, 2002.
32. Lipecki T, Jamińska-Gadomska P, Bęc J, Błazik-Borowa E. In-situ measurements of wind action on scaffoldings. In: 7th Eur. Conf. Wind Eng, 2017, p. #180.
33. Błazik-Borowa E, Robak A. Numerical models of scaffolding decks and their applications. Int J Civ Eng. 2017;15:979–89.
34. Jaminska-Gadomska P, Bęc J, Lipecki T, Robak A. Verification of the façade scaffolding computer model. Arch Civ Eng. 2018;64:41–53. https://doi.org/10.2478/ace-2018-0003.